Desalination and Water Treatment
www.deswater.com
doi: 10.1080/19443994.2015.1110726

57 (2016) 15714–15723
July

Taylor & Francis
Taylor & Francis Group

Application of nanoscale iron oxide-hydroxide-impregnated activated carbon (Fe-AC) as an adsorbent for vanadium recovery from aqueous solutions

Hakimeh Sharififard, Mansooreh Soleimani*, Farzin Zokaee Ashtiani

Department of Chemical Engineering, Amirkabir University of Technology, No. 424, Hafez Ave, P.O. Box 15875-4413, Tehran, Iran, email: h.sharififard@aut.ac.ir (M. Soleimani), Tel. +98 21 64543152; Fax: +98 21 66405847; emails: Soleimanim@aut.ac.ir (H. Sharififard), zokaee@aut.ac.ir (F. Zokaee Ashtiani)

Received 23 April 2015; Accepted 10 October 2015

ABSTRACT

In this study, iron oxide-hydroxide-impregnated activated carbon (Fe-AC) nanocomposites were prepared as new adsorbents for vanadium recovery from aqueous solutions. The commercial activated carbon was modified via a permanganate/ferrous iron synthesis method. The influences of main synthesis parameters, such as temperature (35–85˚C), time (5–24 h), and $FeSO_4$ concentration (0.2–0.6 mol L^{-1}), were investigated to obtain the best adsorbent for vanadium recovery. The effects of these parameters were optimized by Taguchi method. The optimal conditions for the synthesis of the best adsorbent were $FeSO_4$ concentration = 0.4 M, time = 24 h, and temperature = 55˚C. The characterization tests showed that the nature of iron nanoparticles on AC surfaces is iron oxide-hydroxide (FeOOH). The results showed that Fe-AC nanocomposite exhibited a reasonable capacity for vanadium recovery from aqueous solutions. According to Langmuir isotherm, maximum adsorption capacities were 37.87 and 119.01 mg g^{-1} for activated carbon and Fe-AC, respectively.

Keywords: Nanoscale iron oxide-hydroxide; Activated carbon; Vanadium recovery

1. Introduction

Activated carbon has been a preferred adsorbent in major industrial applications for many years, especially in water and wastewater treatment processes due to its high adsorption capacity, high adsorption rate, and good resistance to abrasion. Activated carbon is also an effective adsorbent for organic materials, but not as effective to adsorb inorganic ions [1,2]. The application of nanoscale metal hydroxide-impregnated activated carbon presents a new method to improve the adsorption capacity of activated carbon for the removal of organic and inorganic pollutants from gas and liquid systems [3–6]. Iron hydroxide is one of the metal hydroxides. Different technologies, such as evaporation of iron salt in presence of activated carbon, iron precipitation with alkaline solutions, and oxidation/precipitation of iron, have been proposed for the attachment of these metal hydroxides onto activated carbon surfaces [7–9]. However, energy consumption for some of these methods is very high [6]. Anchorage is a simple method for the synthesis of nanoscale iron hydroxide-impregnated activated

---

*Corresponding author.

Presented at the 3rd International Conference on Water, Energy and Environment (ICWEE)
24–26 March 2015, Sharjah, United Arab Emirates

carbon nanocomposite, which consists of using a solution of iron salt [10,11].

Vanadium is a very important metal from an economical and environmental point of view. Vanadium is a well-known toxic metal and exists in environment as tetravalent [V(IV)] and pentavalent [V(V)] forms of which the pentavalent form is the more toxic one [12–14]. The Occupational Safety and Health Administration (OSHA) has determined that exposure to vanadium pentoxide dust and vanadium fumes should be limited to 0.5 and 0.1 mg m^{-3}, respectively, during an 8 h working day [14]. This metal is widely used in many industries, such as glass, steel, textile, ceramic, photography, metallurgy and plants, that produce industrial inorganic chemicals and pigments. Vanadium has been discharged into the environment from oil refineries and power plants in the form of vanadium-rich oil fuel and coal. Due to environmental risks and economic issues, it is necessary to recover vanadium from industrial effluents such as steel and oil slags. Different technologies, such as extraction, membrane technology, and adsorption, have been studied to separate vanadium from wastewater [14–23]. The adsorption technology is more advantageous due to its high separation efficiency, low cost, and easy operation.

Since the adsorption capability of activated carbon is low for inorganic materials such as vanadium, iron oxide-hydroxide-impregnated activated carbon (Fe-AC) nanocomposites were synthesized and used in this work vanadium recovery from aqueous solutions.

Based on the literature review, few research papers have been focused on the application of iron nanoparticles and activated carbon composite as an adsorbent for different separation processes. The synthesis condition of these nanocomposites was different in research works [3,5,6,10,11]. Therefore, the main objective of this study was to synthesize this nanocomposite via simple and low-temperature method and investigate the effects of synthesis condition on adsorption ability of this nanocomposite for vanadium recovery.

2. Materials and methods

2.1. Materials

The activated carbon used in this work is a commercial product manufactured by Norit (the Netherlands) with the trade name Norit ROY 0.8. The size of activated carbon was 300–500 μm (mesh no. 35–50). Ferrous sulfate ($FeSO_4 \cdot 7H_2O$), potassium permanganate ($KMnO_4$), vanadium pentoxide (V_2O_5), sodium hydroxide (NaOH), and sulfuric acid (H_2SO_4) were purchased from Merck company. The solution was prepared using ultrapure deionized (DI) water (18.3 MΩ cm) produced by Milli-Q water purification system (Elix 3 UV (120 V/60 Hz), Millipore).

2.2. Preparation of Fe-AC nanocomposite

Initially, 10 g of activated carbon (AC) was gently mixed with 100 mL of 0.2 M $KMnO_4$ for 20 min. The permanganate-treated AC was then rinsed repeatedly with ultrapure water until all the permanganate was removed, which was verified with no detectable pink/purple color in the washed water. Preparation of the Fe-AC consisted of placing 0.5 g of rinsed AC in contact with 10 mL $Fe(SO_4) \cdot 7H_2O$ solution with certain concentration (M) inside a sealed glass container. The glass container was then placed in a shaker incubator (NB-205, N-BIOTECK) at the desired temperature for a certain period of time (h). Finally, the mixture was filtered with filter paper (Whatman No. 42) and the Fe-AC nanocomposite was rinsed with distilled water until all the soluble iron and iron particles that were not anchored to the carbon surface were separated. To ensure the separation of soluble iron, the iron content of washing water was analyzed using an atomic absorption spectrophotometer (AAS) (Varian AA240). The prepared Fe-AC was dried in an air oven at 60°C for 24 h.

2.3. Experimental design for the synthesis of Fe-AC samples

In this study, the effects of three main synthesis parameters were studied: $Fe(SO_4)$ concentration, contact time, and temperature. The Taguchi method [24] was used for experimental design and the effectiveness of these parameters, as well as the optimum operating conditions for the synthesis of the best adsorbent for vanadium recovery, were determined. Taguchi method leads to the process development by provide a simple, systematic, and efficient approach for conducting experiment during research and development to determine near-optimum settings of design parameters with a few experimental runs. This methodology helps reduce the cost and time [24].

Table 1
Synthesis parameters and their levels

Parameter	Level 1	Level 2	Level 3
$FeSO_4$ conc. (M)	0.2	0.4	0.6
Contact time (h)	5	14	24
Temp. (C)	35	55	85

Table 2
Arrangement of parameters in L9 orthogonal array

Parameters	$Fe(SO_4)$ conc. (M)	Contact time (h)	Temp. (C)	Recovery percent
Experiment				
1	0.2	5	35	77
2	0.2	14	55	88
3	0.2	24	85	90
4	0.4	5	55	100
5	0.4	14	85	96
6	0.4	24	35	90
7	0.6	5	85	96
8	0.6	14	35	87
9	0.6	24	55	100

These operation parameters and their levels are listed in Table 1. The degree of freedom related to three sets of three-level parameters is six and the standard orthogonal array L9, with three columns, and nine rows could be applied for these experiments in accordance with Taguchi method [24]. The experimental layout for these parameters using the L9 orthogonal array is reported in Table 2. The order of experiments was chosen randomly in order to block noise sources. To test the predicted results, confirmation experiments were carried out twice at the same working conditions.

2.4. Adsorption experiments

The Fe-AC samples were used for vanadium recovery from an aqueous solution, and vanadium recovery percentage was selected as the performance characteristic of the synthesis process with the optimum operating conditions determined based on this parameter. The operating conditions were selected based on our previous works [27]. Vanadium recovery experiments were carried out in a batch system at pH 4.5 and 25˚C. Each batch consisted of 0.2 g Fe-AC that was added to 50 mL of vanadium solution (70 mg L^{-1})

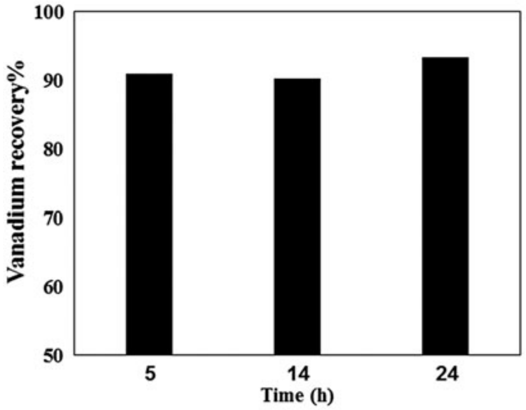

Fig. 2. Effect of contact time (h) on vanadium recovery by nanoscale Fe-AC nanocomposite.

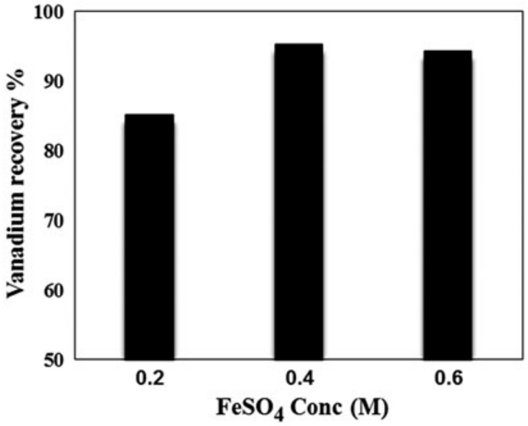

Fig. 1. Effect of $FeSO_4$ Conc. (M) on vanadium recovery by nanoscale Fe-AC nanocomposite.

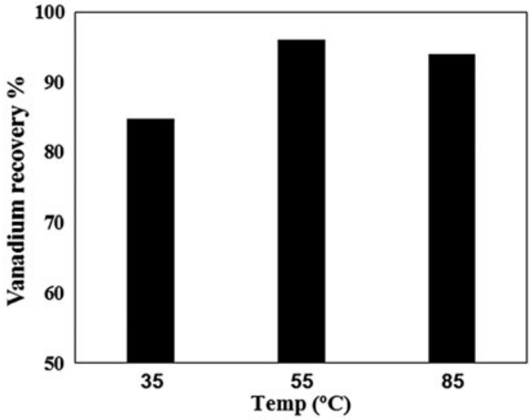

Fig. 3. Effect of temperature (˚C) on vanadium recovery by nanoscale Fe-AC nanocomposite.

Table 3
Results of ANOVA table for the synthesis of nanoscales Fe-AC composite

Synthesis parameters	Sum of squares	Var (*V*)	*F*-ratio	Contribution percentage
$FeSO_4$ conc. (M)	194.9	97.44	67.57	44.41
Contact time (h)	14.89	7.44	5.162	2.778
Temp. (C)	219.6	109.8	76.12	50.13
Error	2.884	1.442		2.67
Total	432.2			100

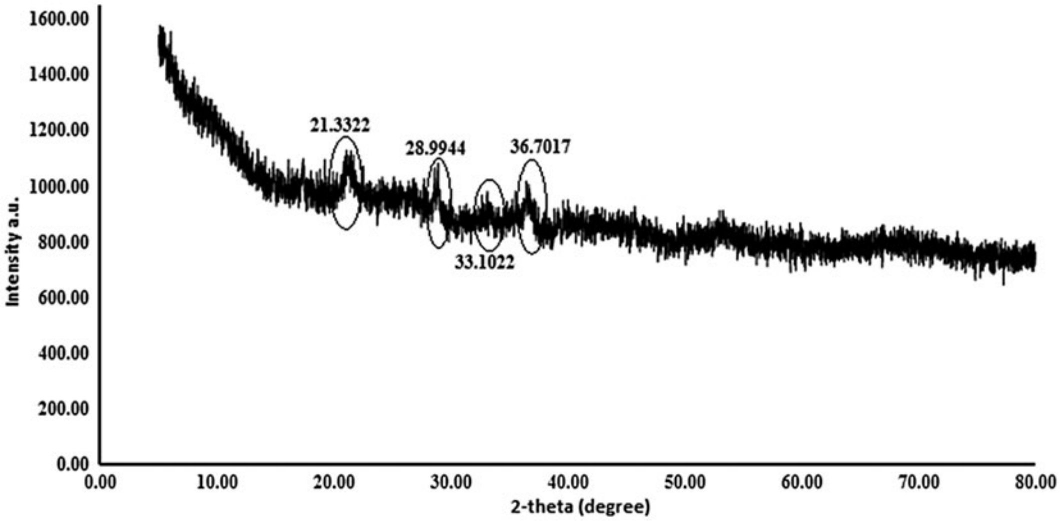

Fig. 4. XRD patterns of Fe-AC nanocomposite.

and stirred at 150 rpm for 3 h. The solution pH was adjusted to 4.5 by adding NaOH and/or H_2SO_4 solutions. The adsorbent was separated by the paper filter (Whatman No. 40) at the end of stirring. The residual vanadium concentration in the solution was determined using AAS (Varian AA240, the wavelength of 318 nm). The percentage of vanadium recovered by Fe-AC was determined from the following equation:

$$\text{Recovery percent} = \frac{(C_0 - C_f)}{C_0} \times 100 \tag{1}$$

In this equation, C_0 and C_f are the initial and final metal ion concentrations (mg L^{-1}), respectively.

2.5. Materials characterization

The iron content in selected Fe-AC samples was determined by using X-ray fluorescence (XRF, unisantis, XMF-104). X-ray diffraction (XRD) spectra of the Fe-AC sample (prepared at optimum conditions) was analyzed using a high-resolution X-ray diffractometer (XRD, Philips X′ Pertdiffractometer, Cu Kα rad).

The average particle size and the morphology of the nanoscale iron oxide-hydroxide particles on activated carbon surface were determined by direct measurement on scanning electron micrographs (SEM, Seron Technology, AIS2100).

The porous texture and surface area of the samples were determined from adsorption−desorption of nitrogen at 77˚K using an automatic volumetric system (Quantachrome NOVA 1000). The surface areas were calculated by applying the BET (Brunauer−Emmett− Teller) method. The volumes (mL g^{-1}) of micropores and mesopores were calculated by HK (Horvath−Kawazoe) and BJH (Barrett, Joyner, and Halenda) methods, respectively [25,26]. The total pore volume for each sample was evaluated from the amount of nitrogen adsorbed at the highest relative pressure, near unity.

2.6. Equilibrium experiments

Equilibrium studies were performed to evaluate the performance of AC and Fe-AC (prepared at optimum condition) for vanadium ions adsorption. In these experiments, 0.05 g of each adsorbent was brought in contact with 50 mL of vanadium ions solution at

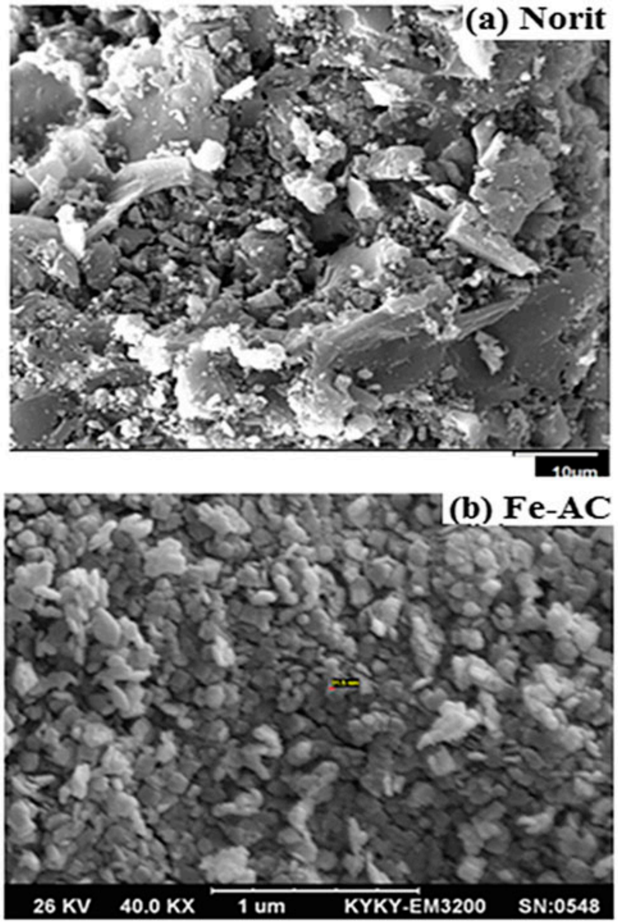

Fig. 5. SEM micrograph of (a) virgin Norit activated carbon and (b) Fe-AC nanocomposite.

different initial concentrations (25–200 mg L^{-1}) and initial pH of 4.5 in a series of flasks. The flasks were agitated on an orbital agitator incubator (N-BIOTECK, NB-205) at 250 rpm for 24 h at 25˚C. After this period, the metal solutions were filtered and the residual concentration of metal ions was determined by AAS. The adsorbed amount of vanadium ions by these adsorbents, q (mg g^{-1}), was determined by Eq. (2):

$$q = \frac{V}{m}(C_0 - C_f) \quad (2)$$

where V and m are the solution volume (L) and dry weight of adsorbent (g), respectively.

3. Results and discussion

3.1. Effect of operating parameters on synthesis of Fe-ACs

As was mentioned earlier, Taguchi method was used to find the optimal synthesis conditions for nanoscale iron oxide-hydroxide-impregnated activated carbon (Fe-AC) to achieve maximum vanadium recovery. The recovery results are presented in Table 2. The data in Figs. 1–3 show the experimental results for vanadium recovery by Fe-AC samples. Fig. 1 indicates that the optimum $FeSO_4$ concentration is 0.4 M. The influence of contact time on vanadium recovery with Fe-AC samples is shown in Fig. 2. As can be seen, an increase in contact time leads to increasing vanadium recovery. It can be suggested that longer contact time tends to increase the iron content of samples by allowing more time for iron

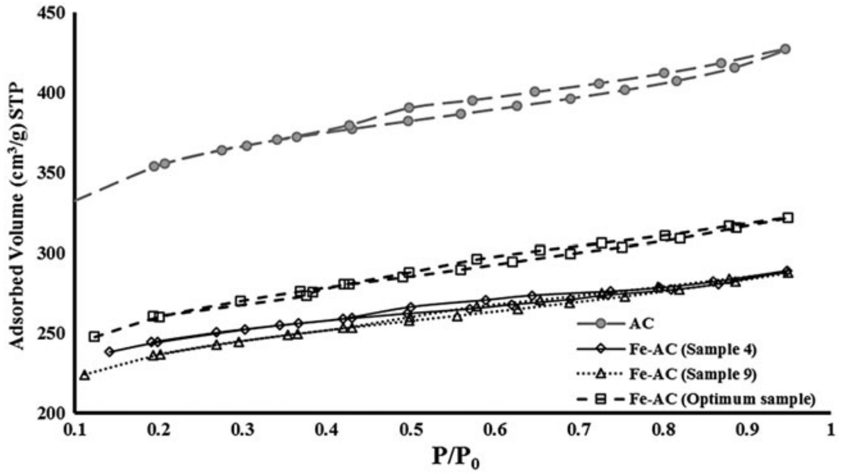

Fig. 6. Adsorption−desorption isotherms of N_2 for adsorbents.

Table 4
Porosity parameters of adsorbents

Adsorbent	BET S.A. ($m^2 g^{-1}$)	V_{tot} ($mL\ g^{-1}$)	V_{micro} ($mL\ g^{-1}$)	V_{meso} ($mL\ g^{-1}$)
AC	1,062.0	0.660	0.530	0.13
Fe-AC (Sample 4)	700.0	0.440	0.370	0.07
Fe-AC (Sample 9)	711.6	0.444	0.356	0.11
Fe-AC (Optimum sample)	777.0	0.500	0.390	0.12

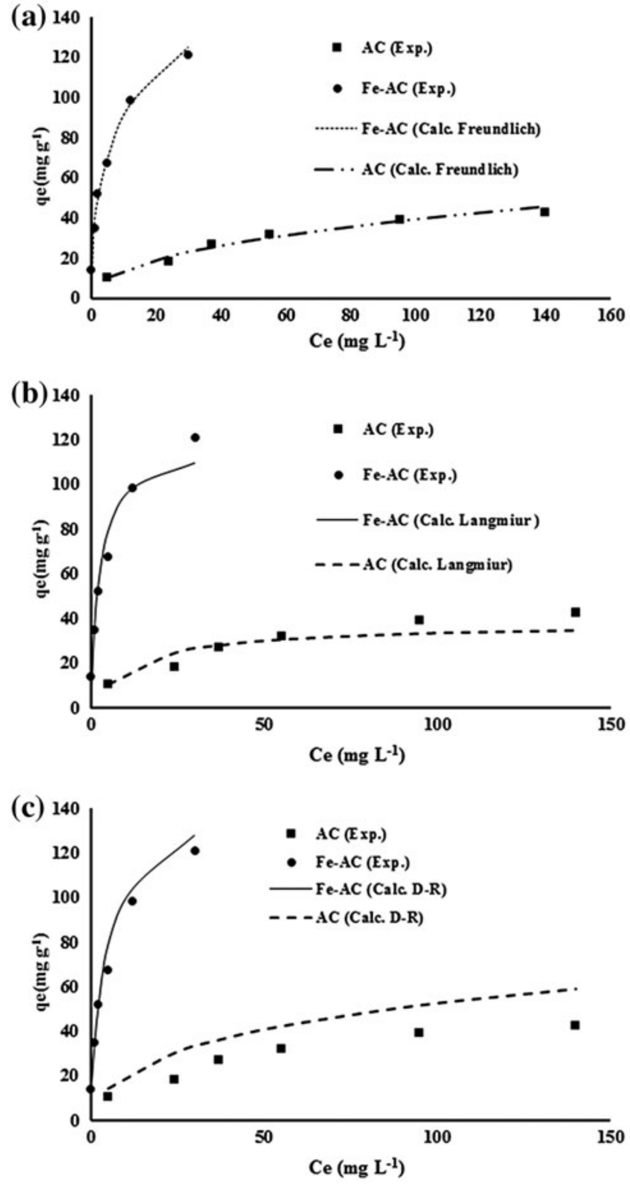

Fig. 7. Equilibrium isotherms of vanadium adsorption on AC and Fe-AC nanocomposites: (a) Freundlich isotherms, (b) Langmiur isotherms, and (c) D–R isotherm.

molecules to diffuse into AC particles. Therefore, more adsorption sites are created on the surface and within the pores of the AC for vanadium adsorption.

The results indicate that the optimum experimental conditions were as follows: concentration of $FeSO_4 = 0.4$ M, contact time = 24 h, and temperature = 55℃. The Fe-AC nanocomposite synthesized at optimum operating condition had the ability to recover almost all vanadium (about 100%) ions from aqueous solutions at these operating conditions after 3 h. The obtained optimum condition is limited to the ranges of selected parameters.

The analysis of variance (ANOVA) table is used in Taguchi method to determine the contribution percentage of each parameter. The *F*-ratio in ANOVA table can be used to determine the parameters that have a significant effect on the performance characteristic. The calculated values of *F*-ratio are compared with F values predicted by statistical *F* distribution (in Fischer tables) [28] at 95% confidence. According to the rule, when the *F* calculated in the ANOVA table is bigger than the standard *F*, the parameter is significantly influenced by the response variable at the respective confidence level.

The results of ANOVA are presented in Tables 3. The data in Table 3 indicates that $FeSO_4$ concentration and temperature were the most significant synthesis process parameters. According to the data in Table 3, the maximum percentage of error for the results is 2.67, which is not significant. From the Fisher tables, the value of *F* with 95% confidence for vanadium recovery by Fe-AC nanoscales composites is: $F_{0.05,2,2} = 19$ (0.05 is probability, 2 and 2 are the degrees of freedom of parameter and error). Based on these values, the *F* calculated in the ANOVA table is bigger than standard *F* for $FeSO_4$ concentration and temperature. Therefore, these parameters have a significant effect on the performance characteristic.

3.2. Characterization of adsorbents

The XRF characterization tests were done for the Fe-AC samples that recovered almost all the vanadium from aqueous solutions (samples 4 and 9, according to Table 2, and Fe-AC prepared at optimum condition). The iron contents of samples 4, 9, and Fe-AC prepared at optimum operation condition were 11.89, 12.57, and 14.25 wt.%, respectively, which indicate that iron-coated AC effectively.

The structure of the iron nanoparticles on AC surface was verified by XRD patterns shown in Fig. 4. This figure shows the nanocrystallite peaks matching well with the standard FeOOH (00-003-0251). The Mn phases (from pretreatment with $KMnO_4$) are involved in the formation of FeOOH nanoparticles [29].

To clearly understand the average particle size and morphology of nanoscale iron oxide-hydroxide on the surface of activated carbon, the Fe-AC sample prepared at optimum conditions was characterized by SEM. Fig. 5 shows the SEM images of Norit virgin-activated carbon and Fe-AC nanocomposite. The figure reveals the presence of berry-like nanoparticles inside the pores and on the surface of Fe-AC media. The size of these nanoparticles ranges from 30 to 80 nm.

Nitrogen adsorption–desorption isotherms for these samples are illustrated in Fig. 6. The results show that the adsorption–desorption isotherms of samples were similar, and it can be concluded that these isotherms belong to the combination of type I and type II in IUPAC classification [30,31]. These types of isotherms can usually be observed in porous materials with a combination of micro and mesopores. The small hysteresis loops of the isotherms are H4 class, which are often associated with narrow slit-like pores with a regular structure [32]. The porosity parameters of the adsorbents have been deduced from N_2 adsorption−desorption data and are reported in Table 4. The results indicate that the formation of iron nanoparticles inside and outside the porous structure of the AC caused a reduction in BET surface area and pore volume (micro and mesopore). The results indicate that the percentage of micropores and mesopores decreased by the formation of nanoparticles on the surface of AC. Therefore, it could be concluded that the molecules of iron oxide-hydroxides diffused into the micro- and mesopore structure of AC and limited the accessibility of N_2 molecules to micro- and mesopores.

3.3. Adsorption equilibrium

The results of adsorption equilibrium experiments of vanadium on AC and Fe-AC adsorbents are illustrated in Fig. 7. Fe-AC nanocomposites exhibited a considerable vanadium adsorption capacity in contrast to AC. These data were fitted by the Langmuir, Freundlich and Dubinin–Radushkevich (D–R) isotherm models. The isotherm equations and parameters are reported in Table 5. Results show that the adsorption equilibrium data fitted well with the Fruendlich isotherm, which may be attributed to the coexistence of different sorption sites, and/or different sorption mechanisms, or sorption of different vanadium species that led to a heterogeneous adsorption. Based on Table 5, the measured adsorption capacities of AC and Fe-AC were 37.87 and 119.01 mg g^{-1}, respectively. This higher capacity of Fe-AC may be related to the availability and particle size of the iron nanoparticles loaded onto AC. These nanoparticles create new positive adsorption sites for vanadium anions on the AC surface.

The maximum vanadium ion adsorption capacity for other adsorbents is listed in Table 6 for a better

Table 5
Equilibrium isotherm parameters for AC and Fe-AC[a]

		Parameters	
Isotherm	Equation	AC	Fe-AC
Langmuir	$\frac{1}{q_e} = \frac{1}{q_{max} \cdot K_L} \cdot \frac{1}{C_e} + \frac{1}{q_{max}}$	q_{max} = 37.870 mg g^{-1} K_L = 0.076 L mg^{-1} R^2= 0.940	q_{max} = 119.010 mg g^{-1} K_L = 0.397 L mg^{-1} R^2 = 0.970
Freundlich	$\log q_e = \frac{1}{n} \log C_e + \log K_f$	n = 2.280 K_f = 5.220 R^2 = 0.990	n = 2.600 K_f = 37.020 R^2 = 0.990
D–R	$\ln q_e = \ln q_m - \beta\varepsilon \quad \varepsilon = RT \ln\left(1 + \frac{1}{C_e}\right)$	β = 4e-9 mol^2 J^{-2} q_m = 0.003 mol g^{-1} R^2 = 0.943	β = 3e-9 mol^2 J^{-2} q_m = 0.008 mol g^{-1} R^2 = 0.981

[a]Description of parameters is presented in notation table.

Table 6
Adsorption capacities of different adsorbents for vanadium ions adsorption

Adsorbent	$q_{\max}$ (mg g^{-1})	Initial pH	Adsorbent dose (g L^{-1})	Initial concentration (mg L^{-1})	Refs.
Protonated chitosan flakes (PCF)	12.22	4.4–5.0	5.0	1–5	[14]
$ZnCl_2$-modifed activated carbon	24.90	4.0–9.0	4.0	40–120	[20]
Fe(III)/Cr(III)hydroxide waste	11.43	4.0	10.0	10–40	[22]
His-MWCNTs	4.85	5.5	0.8	1–8	[23]
Crosslinked chitosan	6.27	4.0–4.5	0.6	–	[33]
Metal sludge	24.80	7.6	10.0	10–50	[34]
Zr(IV)-impregnated collagen fiber	137.96	5.0	1.0	100–600	[35]
PGTFS–$NH_3^+Cl^-$	45.86	6.0	2.0	10–300	[36]
Calcined Mg/Al hydrotalcite	513.00	3.0	0.2	10–50	[37]
Zr(IV)-loaded orange juice residue	51.90	2.5	2.0	–	[38]
AC	37.78	4.5	1.0	25.0–200.0	This work
Fe-AC	119.01	4.5	1.0	25.0–200.0	This work

comparison [14,20,22,23,33–38]. This comparison indicates that AC and Fe-AC adsorbents exhibit a reasonable adsorption capacity for vanadium adsorption from aqueous solution.

Based on D–R isotherm parameters, the mean free energy E (kJ mol^{-1}) (calculated from Eq. (3)) of adsorption per molecule of the adsorbate were 11.180 and 12.909 kJ mol^{-1} for AC and Fe-AC, respectively, suggesting that the process under consideration had a markedly chemical nature (chemisorption), rather than being a pure physical adsorption [20].

$$E = \frac{1}{(2\beta)^{1/2}} \tag{3}$$

4. Conclusion

The main purpose of this work was to synthesize an effective adsorbent for vanadium recovery from aqueous solutions. The study demonstrated that the impregnation approach using the permanganate/ferrous iron solution was an effective method to anchor nanoscale iron oxide-hydroxide particles onto granular activated carbons. The Taguchi analysis showed that the optimum synthesis conditions were: $FeSO_4$ concentration = 0.4 M, contact time = 24 h, and temperature = 55°C. The ANOVA results indicated that the $FeSO_4$ concentration and temperature had significant effect on the performance characteristic. The Fe-AC synthesized at optimum condition could recover almost 100% of vanadium from the aqueous solution after 3 h. The particle size of iron oxide-hydroxide impregnated on activated carbon surface was in the range of 30–80 nm. The adsorption equilibrium data fitted well with the Fruendlich isotherm.

Acknowledgement

The authors gratefully acknowledge that they received financial support in the form of a research grant (research project No. 61736) from the Iran nanotechnology initiative council, Iran. The authors sincerely thank Mrs. Doustmohammadi for analyzing the samples by AAS.

Notation table

$q_{\max}$	—	maximum adsorption capacity of adsorbent (mg g^{-1})
K_L	—	Langmuir constant related to energy of adsorption (L mg^{-1})
n	—	Freundlich–exponent related to adsorption intensity
K_f	—	Freundlich constant related to adsorption capacity of the adsorbent ($mg^{1-(1/n)}$ $L^{1/n}$ g^{-1})
q_m	—	theoretical saturation capacity (mol g^{-1})
β	—	constant term related to the mean free energy of adsorption per mole of the adsorbate (mol^2 J^{-2})
R	—	the universal gas constant (8.314 J mol^{-1} K^{-1})
T	—	the absolute temperature (K)

References

[1] R. Chand Bansal, M. Goyal, Activated Carbon Adsorption, CRC Press, Taylor & Francis Groups, Boca Raton, FL, 2005.

[2] H. Marsh, F. Rodriguez Reinoso, Activated Carbon, Elsevier, Amsterdam, 2006.

[3] J.A. Arcibar-Orozco, J.R. Rangel-Mendez, T.J. Bandosz, Reactive adsorption of SO_2 on activated carbons with deposited iron nanoparticles, J. Hazard. Mater. 246–247 (2013) 300–309.

[4] N. Yang, S. Zhu, D. Zhang, S. Xu, Synthesis and properties of magnetic Fe_3O_4-activated carbon nanocomposite particles for dye removal, Mater. Lett. 62 (2008) 645–647.

[5] M.H. Do, N.H. Phan, T. Dung-Nguyen, T.T. Suong Pham, V.K. Nguyen, T.T.T. Vu, T.K. Phuong-Nguyen, Activated carbon/Fe_3O_4 nanoparticle composite: Fabrication, methyl orange removal and regeneration by hydrogen peroxide, Chemosphere 85 (2011) 1269–1276.

[6] B. Kakavandi, R. Rezaei Kalantary, A. Jonidi Jafari, S. Nasseri, A. Ameri, A. Esrafili, A. Azari, Pb(II) adsorption onto a magnetic composite of activated carbon and super paramagnetic Fe_3O_4 nanoparticles: Experimental and modeling study, Clean—Soil Air Water 43 (2015) 1157–1166.

[7] C.S. Castro, M.C. Guerreiro, L.C.A. Oliveira, M. Gonçalves, A.S. Anasta´ cio, M. Nazzarro, Iron oxide dispersed over activated carbon: Support influence on the oxidation of the model molecule methylene blue, Appl. Catal. A: Gen. 367(1–2) (2009) 53–58.

[8] H. Zhu, Y. Jia, X. Wu, H. Wang, Removal of arsenic from water by supported nano zero-valent iron on activated carbon, J. Hazard. Mater. 172(2–3) (2009) 1591–1596.

[9] E. Deliyanni, T.J. Bandosz, Importance of carbon surface chemistry in development of iron-carbon composite adsorbents for arsenate removal, J. Hazard. Mater. 186(1) (2011) 667–674.

[10] J.H. Xu, N.Y. Gao, Y. Deng, S.Q. Xia, Nanoscale iron hydroxide-doped granular activated carbon (Fe-GAC) as a sorbent for perchlorate in water, Chem. Eng. J. 222 (2013) 520–526.

[11] H.S. Park, J.R. Koduru, K.H. Choo, B. Lee, Activated carbons impregnated with iron oxide nanoparticles for enhanced removal of bisphenol A and natural organic matter, J. Hazard. Mater. 286 (2015) 315–324.

[12] H. Wyers, Some toxic effects of vanadium pentoxide, Brit. J. Ind. Med. 3 (1946) 177–182.

[13] B. Patel, G.E. Henderson, S.J. Haswell, R. Grzeskowiak, Speciation of vanadium present in a model yeast system, The Analyst 115 (1990) 1063–1066.

[14] A. Padilla-Rodríguez, J.A. Hernández-Viezcas, J.R. Peralta Videa, G.L. Gardea Torresdey, O. Perales Pérez, F.R. Román Velázquez, Synthesis of protonated chitosan flakes for the removal of vanadium(III, IV and V) oxyanions from aqueous solutions, Microchem. J. 118 (2015) 1–11.

[15] L.J. Lozano, C. Godınez, Comparative study of solvent extraction of vanadium from sulphate solutions by primene 81R and alamine 336, Miner. Eng. 16 (2003) 291–294.

[16] L.D. Kurbatova, D.I. Kurbatov, Extraction recovery of vanadium(V) from sulfuric acid solutions, Russ. J. Appl. Chem. 79 (2006) 850–852.

[17] M. Alibrahim, H. Shlewit, S. Alike, Solvent extraction of vanadium(IV) with di(2-ethylhexyl) phosphoric acid and tributyl phosphate, Chem. Eng. J. 52(1) (2008) 29–33.

[18] L.J. Lozano, C. Godínez, F.J. Alguacil, Facilitated transport of vanadium(V) by supported liquid membranes, Hydrometallurgy 80 (2005) 196–202.

[19] M. Nabavinia, M. Soleimani, A. Kargari, Vanadium recovery from oil refinery sludge using emulsion liquid membrane technique, Int. J. Chem. Environ. Eng. 3 (2012) 149–152.

[20] C. Namasivayam, D. Sangeetha, Removal and recovery of vanadium(V) by adsorption onto $ZnCl_2$ activated carbon: Kinetics and isotherms, Adsorption 12 (2006) 103–117.

[21] H. Sharififard, M. Soleimani, M. Nabaviniaand, M. Songolzadeh, Vanadium recovery from synthetic wastewater by adsorption onto Chitosan, The 2011 International Conference on Water, Energy and Environment (ICWEE2011), Sharjah, United Arab Emirates, November 14–17, 2011.

[22] K. Prathap, C. Namasivayam, Adsorption of vanadate (V) on Fe(III)/Cr(III) hydroxide waste, Environ. Chem. Lett. 8 (2010) 363–371.

[23] Y. Liu, Y. Li, L. Yang, Histidine functionalized multi-walled carbon nanotubes as sorbent for flow injection-electrothermal atomic absorption spectrometric ultrasensitive determination of trace vanadium(V) in biological and environmental samples, Microchem. J. 104 (2012) 56–61.

[24] D.C. Montgomery, Design and Analysis of Experiments, third ed., Wiley, New York, NY, 1991.

[25] S. Lowell, J.E. Shields, M.A. Thomas, M. Thommes, Characterization of Porous Materials and Powders: Surface Area, Pore Size and Density, Dordrecht, Springer, 2004.

[26] F.B. Aarden, Adsorption onto Heterogeneous Porous Materials: Equilibria and Kinetics. Ph.D. Dissertation, Technische Universiteit, Eindhoven, Eindhoven, 2001.

[27] H. Sharififard, M. Soleimani, Optimization of vanadium removal with activated carbon using response surface methodology, 2nd International Conference on Chemistry Engineering and Chemical Process (ICCC2014), Istanbul, Turkey, July, 10–11, 2014.

[28] R.A. Fischer, Statistical Methods for Research Workers, Oliver & Boyd, London, 1925.

[29] A.M. Cooper, K.D. Hristovski, T. Möller, P. Westerhoff, P. Sylvester, The effect of carbon type on arsenic and trichloroethylene removal capabilities of iron (hydr)oxide nanoparticle-impregnated granulated activated carbons, J. Hazard. Mater. 183 (2010) 381–388.

[30] S.J. Gregg, K.S. Sing, Adsorption, Surface Area, and Porosity, Academic Press, New York, NY, 1982.

[31] K.S.W. Sing, Reporting physisorption data for gas/solid systems with special reference to the determination of surface area and porosity, Pure. Appl. Chem. 57 (1985) 603–619.

[32] J.H. Chua, The adsorption of fatty acids using metal silica complexes from rice husk ash. Master's Dissertation, Universiti Sains Malaysia, Penang, 2008.

[33] S. Qian, H. Wang, G. Huang, S. Mo, W. Wei, Studies of adsorption properties of crosslinked chitosan for vanadium(V), tungsten(VI), J. Appl. Polym. Sci. 92 (2004) 1584–1588.

[34] A. Bhatnagar, A. Kumar Minocha, D. Pudasainee, H.K. Chung, S.H. Kim, H.S. Kim, G. Lee, B. Min, B.H. Jeon, Vanadium removal from water by waste metal sludge and cement immobilization, Chem. Eng. J. 144 (2008) 197–204.

[35] X.P. Liao, W. Tang, R.Q. Zhou, B. Shi, Adsorption of metal anions of vanadium(V) and chromium(VI) on Zr(IV)-impregnated collagen fiber, Adsorption 14 (2008) 55–64.

[36] T.S. Anirudhan, P.G. Radhakrishnan, Adsorptive performance of an amine-functionalized poly(hydroxyethylmethacrylate)-grafted tamarind fruit shell for vanadium(V) removal from aqueous solutions, Chem. Eng. J. 165 (2010) 142–150.

[37] T. Wang, Z. Cheng, B. Wang, W. Ma, The influence of vanadate in calcined Mg/Al hydrotalcite synthesis on adsorption of vanadium(V) from aqueous solution, Chem. Eng. J. 181–182 (2012) 182–188.

[38] Q. Hu, H. Paudyal, J. Zhao, F. Huo, K. Inoue, H. Liu, Adsorptive recovery of vanadium(V) from chromium (VI)-containing effluent by Zr(IV)-loaded orange juice residue, Chem. Eng. J. 248 (2014) 79–88.